



1 **Updated atmospheric mercury emissions from iron and**
2 **steel production in China during 2000-2015**

3 **Qingru Wu^{1,2}, Wei Gao^{1,2}, Shuxiao Wang^{1,2*}, Jiming Hao^{1,2}**

4 ¹School of Environment, and State Key Joint Laboratory of Environment Simulation and
5 Pollution Control, Tsinghua University, Beijing 100084, China

6 ²State Environmental Protection Key Laboratory of Sources and Control of Air Pollution
7 Complex, Beijing 100084, China

8 *Correspondence to:* S. X. Wang (shxwang@tsinghua.edu.cn)



9 **Abstract**

10 Iron and steel production (ISP) is one of the significant atmospheric Hg emission sources
11 in China. Atmospheric mercury (Hg) emissions from ISP during 2000-2015 were estimated by
12 using a technology-based emission factor method. To support the application of this method,
13 databases of Hg concentrations in raw materials, technology development trends, and Hg
14 removal efficiencies of air pollution control devices (APCDs) were constructed through
15 national sampling and literature review. Hg input to ISP increased from 21.6 t in 2000 to 94.5
16 t in 2015. In the various types of raw materials, coking coal and iron concentrates contributed
17 41%-55% and 22%-30% of the total Hg input. Atmospheric Hg emissions from ISP increased
18 from 11.5 t in 2000 to 32.7 t in 2015 with the peak of 35.6 t in 2013. During the study period,
19 although sinter/pellet plant and blast furnace were the largest two emission processes,
20 emissions from roasting plant and coke oven accounted for 22%-34% of ISP's emissions,
21 which indicated that attention should also be paid on the emissions from these processes when
22 estimating ISP's emissions. Overall Hg speciation shifted from 50/44/6 (gaseous elemental
23 Hg (Hg^0) / gaseous oxidized Hg (Hg^{II}) / particulate-bound Hg (Hg_p)) in 2000 to 40/59/1 in
24 2015, which indicated higher proportion of Hg deposition around the emission points. In the
25 coming years, emissions from ISP are expected to decrease due to the projection of decreasing
26 steel productions, increasing energy consumption efficiency, and improvement of APCDs.
27 With the coming of high-yield-period of steel scrap production, the increasing application
28 proportion of short process steel making method will not only reduce Hg emissions, but also
29 increase the emission proportion of Hg^0 .

30
31



32 **1 Introduction**

33 China is the largest iron and steel production (ISP) country in the world. Crude steel
34 production has increased from 127 Mt in 2000 to 804 Mt in 2015 (CISIA, 2001-2016). Rapid
35 growth of ISP has led to large emissions of air pollutants including mercury (Hg) (Wang K. et
36 al., 2016). To reduce Hg pollution, it is important to quantify atmospheric Hg emissions from
37 ISP.

38 According to existing national inventories, atmospheric Hg emissions from ISP
39 increased from 4.9 t in 1999 to 25.5 t in 2010 (AMAP/UNEP, 2008; Streets et al., 2005; Wu et
40 al., 2006; Zhang L. et al., 2015). In these studies, Hg emissions were determined as the
41 product of crude steel production and unique emission factor of 0.04 g/t steel produced. Later
42 long-term emission inventories revised the unique emission factor with dynamic factors by
43 adopting transformed normal distribution function (Tian et al., 2015; Wang K. et al., 2016;
44 Wu et al., 2016). Such method was based on the assumption that the emission factor was
45 gradually improved according to the simulation curve and attempted to simulate the impact of
46 technology improvement and pollution control on emission factor variation. However, the
47 emission factors actually did not link with technology and APCDs directly. Thus, the
48 simulated emission factors may be quite different from actual situation during a certain
49 short-term period (e.g. ten years) when technology and APCDs experienced dramatic change
50 (Wu et al., 2016), especially under the background of tightening requirement of
51 environmental protection in China in the past decades (MEP, 2011; NEA, 2014; SC, 2013).
52 Recent global assessment report applied a technology-based emission factor method for
53 global ISP including China's (AMAP/UNEP, 2013). However, most of the parameters which
54 were used to calculate the emission factors were from developed countries, which may impact
55 the accuracy of emissions from developing countries such as China. In addition, emissions
56 due to the use of steel scrap were not calculated in the report. With the coming of
57 high-yield-period (after 2020) of steel scrap production in China (Guo and Wei, 2010),
58 emissions due to the consumptions of steel scrap cannot be ignored.

59 The dominant parameters of a technology-based emission factor included Hg removal
60 efficiencies of APCDs and Hg concentrations in raw materials (Wu et al., 2016; Wu et al.,



61 2012; Zhang L. et al., 2015). As to Hg removal efficiencies of APCDs, we hypothesized that
62 the use of data from recent filed experiments on atmospheric Hg emission characteristics in
63 China's ISP will provide a foundation for the technology-based emission factor model (Wu et
64 al., 2016; Wu et al., 2012; Zhang L. et al., 2015). However, current studies cannot support the
65 construction of Hg concentration databases for raw materials. Various raw materials were
66 used in ISP, covering iron concentrates, iron block, alloy materials, steel scrap, coal, and
67 additives (mainly limestone and dolomite). Field experiments in three China's steel smelters
68 indicated that the concentration of iron concentrates was in the range of 23-66 ng/g (Wang F.
69 Y. et al., 2016a; Zhang L. et al., 2015). However, the Hg concentration data from limited
70 samples may lead to large uncertainty of the national inventory. Large studies have reported
71 Hg concentrations in coal (Swaine, 1992; Tian et al., 2010; USGS, 2004; Zhang et al., 2012).
72 But the specific requirement of low-sulfide coal (less than 1.2%) may make the Hg
73 concentration in the consumed coal in ISP different from previous databases (Tao and Wang,
74 1994), since low-sulfide coal was generally accompanied by low-Hg (Zhang, 2012). Rarely
75 studies have reported Hg concentrations in steel scrap and dolomite. Therefore, constructing
76 Hg concentration databases of raw materials was the base to apply a technology-based
77 emission factor model for China's ISP.

78 In this study, a technology-based emission factor model was constructed to estimate
79 atmospheric Hg emissions from China's ISP. To fulfill this aim, raw materials consumed in
80 steel smelters have been sampled and Hg concentrations have been analyzed to construct the
81 Hg concentration databases. Up-to-date Hg removal efficiencies from field experiments and
82 the development trends of production technology and APCDs have been summarized to
83 support the application of emission factor model.

84 2 Methodology

85 2.1 Technology-based emission factor model for ISP

86 Generally speaking, ISP method included long process steel making method and short
87 process steel making method. The long process steel making method included roasting plant,
88 coke oven, sinter/pellet plant, blast furnace, and oxygen steel making (**Fig. 1**). The short



89 process steel making method produced crude steel in arc steel making process directly.

90 Thus, atmospheric Hg emissions from ISP by province can be calculated as follows.

$$\begin{aligned} E_i(t) &= E_{i,l}(t) + E_{i,s}(t) \\ &= E_{i,l,r}(t) + E_{i,l,c}(t) + E_{i,l,p}(t) + E_{i,l,b}(t) + E_{i,l,o}(t) \\ &\quad + E_{i,s,a}(t) \end{aligned} \quad (\text{E1})$$

91 where, E was atmospheric Hg emissions from ISP, t ; i was province; t referred to studied
92 year; l and s referred to long and short process steel making method; r , c , p , b , o , a referred to
93 roasting plant, coke oven, sinter/pellet plant, blast furnace, oxygen steel making, and arc steel
94 making.

95 For each process x , the technology-based emission factor and speciated Hg emissions
96 can be calculated as follows.

$$EF_{i,x,k}(t) = \sum_j C_{i,x,j} \times M_{i,x,j}(t) \times S_i(t)^{-1} \times \gamma_x \times \sum_m \theta_m(t) \times \delta_{k,m} \times (1 - \eta_m) \times 1000^{-1} \quad (\text{E2})$$

$$E_{i,x,k}(t) = EF_{i,x,k}(t) \times S_i(t) \quad (\text{E3})$$

97 where, EF was emission factor, g/t; x was studied process; k was speciated Hg; j was the
98 type of consumed raw material; C was Hg concentration in the consumed raw material, ng/g
99 (see section 2.2.1); M was the consumption of raw material, Mt (see section 2.2.2); S was the
100 production of crude steel, Mt (see section 2.2.2). γ was Hg release rate, which meant the
101 percentage of Hg released to flue gas from raw material, %. Hg release rate were collected
102 from filed experiment studies (**Table S1**). That was 98% for roasting plant, 80% for coke
103 oven, 85% for sinter/pellet plant, 98% for blast furnace, 80% for oxygen steel making furnace,
104 and 95% for arc steel making furnace. m referred to the type of APCD combination (see
105 section 2.2.3); δ was the proportion of different Hg speciation (see section 2.2.3), %; θ was
106 the application rate of different APCD combinations (see section 2.2.3), %; η was Hg removal
107 efficiency (see section 2.2.3), %.

108 2.2 Parameters for model

109 2.2.1 Hg concentrations in raw materials

110 For the long process steel making method, the dominant raw materials included iron



111 concentrates, iron block, coal, limestone, dolomite, alloy, and steel scrap (**Fig. 1**). In the
112 roasting plant, limestone and dolomite were roasted together or separately to make quick lime
113 and caustic dolomite. In the coke oven, washed coal was used to produce coke. In the
114 sinter/pellet plant, iron-containing materials (mainly iron concentrates), quick lime, caustic
115 dolomite, and produced coke were mixed to produce sintered/pellet block, which were used as
116 raw materials with coal and produced coke in the blast furnace. The produced pig iron from
117 blast furnace and additional scraps were used to produce steel in the oxygen steel making
118 processes. For the short process steel making method, arc steel making process was applied to
119 produce steel by mainly using scraps as raw materials. In each process, Hg input due to the
120 use of intermediated products (e.g., quick lime, caustic dolomite, and coke) was calculated by
121 using mass balance method (Wu et al., 2012).

122 National sampling and Hg concentration analysis were conducted to construct the Hg
123 concentration databases for the consumed raw materials. The sampling, preparation and
124 analysis methods were described in detail in our previous studies (Wu et al., 2012; Zhang et
125 al., 2012). Lumex 915M + pyro attachment (with a detection limit of 0.5 ng/g) was applied to
126 analyze Hg concentration by using U.S. EPA Method 7473 (US EPA, 1998). Number of
127 samples and Hg concentrations in dominant raw materials by province were shown in **Table 1**.
128 National Hg concentrations (median value) in the consumed iron ore were 20 (0.6-387) ng/g,
129 which were lower than the median value of 30 (0.6-600) ng/g used in the global assessment
130 report (AMAP/UNEP, 2013). Overall Hg concentrations in the consumed coking coal (82
131 ng/g) and pulverized coal injection (PCI) coal (73 ng/g) were lower than the 170 (8-2248)
132 ng/g (Zhang, 2012) used in China's coal combustion sectors but higher than the 55 (50-60)
133 ng/g of global assessment report. Hg concentrations in the limestone were 18 (0.9-2753) ng/g.
134 Although the median value was lower than value of 30 (20-50) ng/g applied in the global
135 assessment report, the variation range was much wider according to our analysis. Hg
136 concentrations (median value) in the dolomite and iron block were 9 ng/g and 19 ng/g. In
137 oxygen and arc steel making processes, the main iron-containing materials were steel scrap,
138 alloy scrap, and pig iron. Hg concentrations (median value) in steel scrap and alloy scrap were
139 48 and 2 ng/g while the concentrations in pig iron were less than detection limit. For province



140 with samples no less than 15, the distribution characteristics of Hg concentrations of the
141 samples were generated by using the batch fit function of Crystalball software. Otherwise, Hg
142 concentrations were assumed to fit normal distribution.

143 2.2.2 Provincial consumptions of raw materials

144 Provincial consumptions of raw materials in 2015 were shown in **Table S2**. National
145 limestone consumptions were converted from quick lime consumptions (Ma, 2011) by using
146 the factor of 1.95 t limestone to produce 1 t quick lime (CISIA, 2001-2016) (**Table S3**).
147 National dolomite consumptions were derived from China steel statistics report (Ma, 1995)
148 according to the production trends of crude steel. The limestone and dolomite can be
149 consumed in the roasting and sinter/pellet plant. In the sinter/pellet plants, additives
150 (including limestone and dolomite) consumptions were approximately 153.9 kg/t sinter
151 produced or 10.5 kg/t pellet produced (CISIA, 2001-2016). We assumed that 88% of the
152 additives were limestone and 12% were dolomite according to filed experiments (Wang F. Y.
153 et al., 2016). The rest of limestone and dolomite were consumed in the roasting plants.
154 Provincial consumptions of limestone and dolomite were distributed according to the
155 proportions of provincial pig iron productions in national production (Table S2). Provincial
156 pig iron productions were collected directly from yearbooks (CISIA, 2001-2016).

157 Provincial coking coal consumptions were converted from provincial coke consumptions
158 (CISIA, 2001-2016). Generally, there were two main types of coke production methods,
159 including machining coke production method and indigenous coke production method. Coal
160 consumptions were 1.35 t to produce 1 t of machining coke or 1.65 t to produce 1 t of
161 indigenous coke (UNEP, 2013; Wang, 1991). The produced cokes were used as raw materials
162 in both sinter/pellet plant and blast furnace. Provincial coke consumptions in blast furnace
163 were converted according coke ratio of 363-388 kg coke per t pig iron produced (CISIA,
164 2001-2016). The rest of cokes were assumed to be consumed in sinter/pellet plant.

165 National iron concentrate consumptions were converted from sinter/pellet productions.
166 Approximately 0.91-0.92 t and 0.96-0.97 t of iron concentrates were needed to produce 1 t
167 sinter and 1 t pellet, respectively (CISIA, 2001-2016). National sinter and pellet productions
168 were obtained directly from yearbooks (CISIA, 2001-2016) and provincial data were



169 converted according to provincial pig iron productions.

170 National PCI coal consumptions in blast furnace were collected from national energy
171 statistical yearbook (NESA, 2001-2016) and the provincial data were converted according to
172 provincial pig iron productions. The iron block consumption in blast furnace were converted
173 from pig iron production by using the factor of 156 kg iron block per t pig iron produced
174 (CISIA, 2001-2016).

175 The steel scrap was consumed in both oxygen and arc steel making process.
176 Consumptions of steel scrap in oxygen and arc steel making process were approximately 59.4
177 and 361.9 kg/t crude steel produced. Alloy consumptions to produce per t crude steel were
178 16-17 kg in oxygen steel making process and 140-156 kg in arc oxygen making process.
179 Oxygen and arc steel productions were collected directly from yearbooks (CISIA, 2001-2016).
180 Based on these ratios, provincial steel scrap and alloy consumptions were converted from
181 provincial crude steel productions.

182 2.2.3 Application rate, Hg removal efficiency, and Hg speciation

183 In the roasting plant, blast furnace, and steel making process, dust collectors such as
184 venturi, cyclone (CYC), wet scrubber (WS), electrostatic precipitator (ESP), and fabric filter
185 (FF) were used for flue gas dedusting. In coke oven process, the coal was firstly washed
186 before consumed and the flue gas was cleaned with dust collectors or with additional washing
187 scrubbers. For flue gas from sinter/pellet plant, they were generally cleaned with dust
188 collectors. Additional flue gas desulfurization towers (FGD) were gradually applied after
189 2010. The application rates of different APCD combinations by process during 2005-2010
190 were collected from previous studies (Wang et al., 2014; Zhao et al., 2013). The data of
191 2000-2004 and 2011-2015 were mainly derived from yearbooks (CISIA, 2001-2016; NBS,
192 2001-2016) (Table S4). Hg removal efficiencies and speciation profiles of APCDs (**Table S4**)
193 were collected from filed experiments and literature on emission studies (Gao, 2016; Wang F.
194 Y. et al., 2016; Zhang L. et al., 2015). The distribution characteristics of Hg removal
195 efficiencies were assumed to fit normal distribution characteristics.



196 2.3 Uncertainty analysis

197 Monte Carlo simulation was introduced to estimate the uncertainty of emissions.
198 Detailed description of the simulation processes has been reported in our previous studies
199 (Hui et al., 2016; Wu et al., 2016; Zhang L. et al., 2015). In this study, the (P50-P10)/P50 and
200 (P90-P50)/P50 values were still regarded as lower and upper limits of uncertainties with 80%
201 confidence degree, where P10, P50, and P90 meant that the probabilities of actual results
202 lower than corresponding values were 10%, 50%, and 90%, respectively.

203 3 Results and Discussion

204 3.1 Hg input trends

205 Hg input to ISP increased from 21.6 t in 2000 to 94.5 t in 2015 (**Fig. 2**). The peak of Hg
206 input was in 2014 when the crude steel production reached the highest value (**Table S1**).
207 During 2000-2014, the average annual growth rate (AAGR) of Hg input was 11% while Hg
208 input reduced by 3% from 2014 to 2015. In the various types of raw materials, coking coal
209 and iron concentrates contributed the largest amount of Hg input, accounting for 35%-46%
210 and 25%-32% of the total, respectively. Hg input due to the use of coking coal increased from
211 9.9 t in 2000 to 33.5 t in 2015. Hg input with iron concentrates increased at AAGR of 12%
212 from 2000 and reached 29.2 t in 2015. The PCI coal brought approximately 6%-9% of Hg to
213 ISP. Hg in the additives (including limestone and dolomite) contributed 12%-18% of total Hg
214 input. Hg in the iron block was in the range of 0.6-3.6 t. Hg input due to the use of steel scrap
215 and alloy was 4.1 t in 2015, accounting for 4% of national total. However, steel scrap and
216 alloy contributed 7% of total crude steel production in 2015 (CISIA, 2016).

217 3.2 Hg emission trends

218 3.2.1 Hg emission trends by process

219 Atmospheric Hg emissions from ISP increased from 11.5 t in 2000 to 32.7 t in 2015 (**Fig.**
220 **3**). The peak of emissions was in 2013 when the emissions reached 35.6 t. In 2015, emissions
221 from long process steel making method and short process steel making were 32.2 t and 0.5 t,
222 accounting for 98.3% and 1.7% of national total, respectively. Thus, emissions from long
223 process steel making were still the dominant source of Hg emissions from China's ISP.



224 Among the processes, emissions from sinter/pellet plant accounted for 42%-49% of annual
225 total. Its emissions increased from 4.8 t in 2000 at the AAGR of 10.1% and reached 15.9 t in
226 2015. Blast furnace was also significant Hg emission process. Its emissions increased from
227 1.9 t in 2000 to 7.9 t in 2015 at AAGR of 10.0%. AAGR for roasting plant and coke oven was
228 8.3% and 1.2%. In 2015, both emissions from roasting plant and coke oven were 3.5 t,
229 respectively.

230 The slower AAGR of Hg emissions (7.2%) than that of crude steel production (13%)
231 reflected the impact on Hg emission reduction due to energy saving and environmental
232 protection in ISP. On one hand, Hg input to produce unitary crude steel decreased from 0.17
233 to 0.12 g/t, which mainly benefited from the improvement of coke production efficiency and
234 energy utilization efficiency of sinter/pellet plant and blast furnace. Since 2004, indigenous
235 coke production method with high coal consumption has been gradually replaced with
236 machine coke production method. The coke ratio in sinter/pellet plant has been reduced from
237 approximately 388 kg/t pig iron produced in 2000 to 363 kg/t in 2015 (CISIA, 2001-2016).
238 On the other hand, the improvement of APCDs increased the overall Hg removal efficiency
239 from 54% in 2000 to 72% in 2015. APCDs for coke oven have shown the largest Hg removal
240 efficiencies (64%-87%) while the improvement of APCDs in sinter/pellet plant contributed
241 most to the rapid Hg reduction speed during 2000-2015. The replacement of CYC and WS
242 with ESP and FF in sinter/pellet plant improved Hg removal efficiency from 21% in 2000 to
243 44% in 2010. The application of FGD in addition to dust collectors was the main driver of Hg
244 reduction in sinter/pellet process during 2011-2015. Hg removal efficiency in sinter/pellet
245 plant was 53% in 2015.

246 3.2.2 Hg emission trends by province

247 Provincial Hg emissions in 2000, 2005, 2010, and 2015 were shown in **Table 2**. In 2000,
248 Shanxi, Shanghai, Henan, Hebei, and Shandong were the top five largest emitters with
249 emissions larger than 1 t. Emissions from these five provinces contributed to 58% of national
250 Hg emissions. Following these five provinces were Liaoning, Beijing, Gansu, Jiangsu, and
251 Jiangxi. Summation of the emissions from all the above ten provinces were 9.0 t, accounting
252 for 78% of national emissions in 2000. At the provincial level, we noted significant



253 differences of Hg emission trends during the past 16 years. The AAGR of provincial Hg
254 emissions varied from -40% to 26%. Negative AAGR existed in Beijing and Shanghai
255 provinces, the two most economically developed regions in China. Hg abatement in these two
256 regions was mainly caused by the reduction of crude steel production, which was transferred
257 to nearby provinces such as Hebei, Zhejiang, Jiangsu, and Shandong. Thus, Hg emissions in
258 these nearby provinces all presented high AAGR of more than 10%. In 2015, the largest five
259 Hg emission provinces were changed to Hebei, Shandong, Henan, Jiangsu, and Shanxi
260 provinces. Emissions from these provinces reached 21.5 t, accounting for 68% of national
261 emissions. Liaoning, Jiangxi, Inner Mongolia, Gansu, and Shanghai were also in the list of the
262 top ten largest emitters.

263 3.2.3 Hg emission trends by species

264 Overall Hg speciation profile of ISP experienced great change during the study period,
265 from 50/44/6 (gaseous elemental Hg (Hg^0)/gaseous oxidized Hg (Hg^{II})/particulate-bound Hg
266 (Hg_p)) in 2000 to 40/59/1 in 2015 (**Fig. 4**). The proportion of Hg^{II} increased 15%, whereas
267 both Hg^0 and Hg_p proportion showed decreasing trend. Such shift indicated higher deposition
268 proportion of Hg around the emission points since Hg^{II} has larger deposition velocity and
269 higher water-solubility. For the long process steel making, Hg speciation profile shifted from
270 49/44/7 in 2000 to 39/60/1. The speciation shift in roasting plants was mainly impacted by the
271 replacement of WS and CYC with FF, which increased the emitted Hg^{II} proportion from 38%
272 to 75%. The replacement of indigenous coke production method with machine coke
273 production method mainly contributed to Hg^{II} proportion increase from 42% to 52% at first.
274 However, the gradual installation of WS in addition to cooler for air pollution control of
275 machine coke production method further washed Hg^{II} and reduced Hg^{II} proportion to 49% in
276 2015. Hg^{II} proportion in the exhaust gas of sinter/pellet plant has increased by 20%. The
277 increase of Hg^{II} proportion in sinter/pellet plant was mainly impacted by the substitute of WS
278 with ESP, FF, ESP+WFGD, or ESP+DFGD+FF which generally emitted gas with higher Hg^{II}
279 proportion (**Table S4**). Increase of Hg^{II} emission proportion in blast furnace was due to higher
280 Hg^{II} emission proportion after FF than venturi. In the oxygen steel making process, Hg
281 speciation profile almost unchanged. For the short process steel making, Hg^0 was the



282 dominant speciation during the whole study period and the proportion of Hg^0 increased from
283 66% in 2000 to 79% in 2015.

284 3.3 Uncertainty analysis

285 In 2015, overall uncertainty of atmospheric Hg emissions from ISP was in the range of
286 (-29%, 77%) (**Fig. 5**). Previous studies in ISP indicated the emission uncertainties of this
287 source were (-80%, 100%) in the study of Zhang et al. (2015) and (-100%, 100%) in the study
288 of Streets et al. (2005) and Wu et al. (2006). The improvement of emission estimation of this
289 study was contributed by better knowledge on the Hg concentrations of raw materials and Hg
290 removal efficiencies of APCDs. In all ISP processes, the largest uncertainties existed in
291 emissions from roasting plant (-59%, 130%) and sinter/pellet process (-45%, 126%). These
292 mainly due to larger distribution range of Hg concentrations in limestone and iron ore as well
293 as Hg removal efficiencies of APCDs. The uncertainties of Hg emissions from other processes
294 were much lower, (-49%, 48%) for coke oven, (-23%, 46%) for blast furnace, (-41%, 27%)
295 for oxygen steel making, and (-60%, 54%) for arc steel making.

296 3.4 Comparison and implications

297 Due to the complicated ISP processes and limitations of data availability, the process
298 combinations included in different emission inventories was divided in to four types (**Fig. 6**)
299 (AMAP/UNEP, 2008, 2013; Wang K. et al., 2016; Wu et al., 2016; Wu et al., 2006; Zhang L.
300 et al., 2015). The first type included sinter plant and blast furnace, which were the basic
301 assumption in the emission inventories of Wu et al. (2003), Zhang L. et al. (2015), and
302 AMAP/UNEP (2005). In these studies, unique emission factor of 0.0400 g/t was applied
303 (**Table S5**) and their emissions were similar in the same inventory year. Our emissions for this
304 process combination were almost the same as above estimations around 2005. However, the
305 gap grew with time when FGD was gradually applied in sinter/pellet plant. Therefore,
306 emission factor for this type of combination was reduced from 0.0527 g/t in 2000 to 0.0296
307 g/t in 2015 (**Table S5**). The second type also consisted of steel making in addition to the first
308 type. Our estimation was much higher than the study of Wang K. et al. (2016) because the
309 emission factors applied in Wang K.'s study were mainly derived from European technical



310 report (EMEP/CORINAIR, 2001; EMEP/EEA, 2013). However, the technology applied in
311 Europe may be better than China's situation. For example, the emission factor of 0.00019 g/t
312 applied for blast furnace with FF was used as best emission factor in Wang K.'s study (2016).
313 However, the combination of WS and venturi scrubber was the dominant APCD type in
314 China's blast furnace (Zhao et al., 2013), Hg removal efficiency of which was lower than that
315 of FF. The third type of process combination also included coke oven as part of ISP in
316 addition to the second type. Lower Hg emissions estimated by AMAP/UNEP (2013) were due
317 to their lower Hg concentration in coal. In addition, although different processes were
318 considered in the report, unique APCDs profile was applied in different process where the
319 application of ESP+FGD reached 55%. However, FGD were mainly installed in sinter/pellet
320 plant but rarely applied in other processes. The fourth type also considered the emissions from
321 roasting process where emissions accounted for 9%-11% of total emissions.

322 The comparison of emissions from different types of process combination in this study
323 indicated the significance of our new inventory. The proportion of emissions from these two
324 processes accounted for 22%-34% of ISP's emissions during the whole study period, which
325 indicated the importance of including emissions from roasting plant and coke oven in the ISP
326 emission inventories. In addition, given the impact of APCDs on the emission estimation,
327 inventories in ISP should also apply distinct APCDs profiles for different processes so as to
328 reduce the uncertainty of inventories. In the inter-annual emission inventories, the
329 technology-based estimation method by linking emissions with technology and APCDs
330 directly has shown its advantage in the discussion of emission trends and quantification of Hg
331 removal due to air pollutants control measures.

332 Based on the comprehensive consideration of dominant parameters (e.g., steel
333 production, air pollution control measures) in the technology-based method and the emission
334 trends from China's ISP during 2000-2015, we expected a decreasing trend of Hg emissions
335 in the coming years. On one aspect, emissions of pollutants are required to be reduced by 15%
336 for ISP before 2020 in China (MIIT, 2016). To fulfill this goal, corresponding emission
337 standards have been issued (Wu, 2013), which will accelerate the applications of improved
338 APCDs. During 2010-2015, the increase of SO₂ emission limits from 1500 mg/m³ to 200



339 mg/m^3 promoted the large-scale application of desulfurization devices in the sinter/pellet plant
340 of ISP. After 2015, ISP will move forward to NO_x control by using related technologies such
341 as selective catalytic reduction (SC, 2013), the synergic Hg removal efficiencies of which
342 have been proved in other industries (Wang et al., 2010). On the other aspect, excess steel
343 production capacity combined with decreasing steel consumption currently will lead to the
344 reduction of steel production, as what we have seen during 2014-2015 (CISIA, 2016; MIIT,
345 2016). The crude steel production trends will thereby substantially reduce Hg input to ISP.
346 Besides, energy consumptions are required to be reduced by more than 10% during the
347 2016-2020 (MIIT, 2016). The improvement of energy efficiency in the main processes will
348 also be one dominant measure to reduce energy consumption (Li et al., 2015), which will
349 reduce fuel consumption and further lead to the reduction of Hg input. In addition, with the
350 coming of high-yield-period of steel scrap production (Guo and Wei, 2010), the application
351 proportion of short process steel making method is expected to increase according to the
352 experiences in developed countries (e.g., Europe), which will indirectly reduce the
353 requirement of steel production from long process steel making method. The replacement of
354 steel production method will also be one driver of Hg emission reduction considering lower
355 Hg emission factors of short process. In addition, since Hg^0 is the dominant Hg speciation
356 from arc steel making process, the emission proportion of Hg^0 is expected to increase.

357 **4 Conclusion**

358 In this study, updated atmospheric Hg emissions from ISP during 2000-2015 were
359 estimated by using technology-based emission factor method with up-to-date parameters. The
360 input of Hg as impurity of raw materials for ISP increased from 21.6 t in 2000 to 94.5 t in
361 2015. In the various types of raw materials, coking coal and iron concentrates contributed to
362 the largest amount of Hg input, 35%-46% and 25%-31% of national total, respectively.
363 Atmospheric Hg emissions from ISP increased from 11.5 t in 2000 to the peak of 35.6 t in
364 2013, and then reduced to 32.7 t in 2015. Overall Hg speciation shift from 50/44/6
365 ($\text{Hg}^0/\text{Hg}^{\text{II}}/\text{Hg}_p$) in 2000 to 40/59/1 in 2015. In the coming years, emissions from ISP are
366 expected to decrease due to the projection of Hg input reduction and improvement of APCDs.

367 In 2015, emissions from long process steel making method and short process steel



368 making were 32.2 t and 0.5 t, accounting for 98.3% and 1.7% of national total, respectively.
369 Sinter/pellet plant and blast furnace were the largest two emission processes, emissions from
370 which accounted for 49% and 24% of national emissions. However, emissions from roasting
371 and coke oven should cause attention because their emissions accounted for 22% of national
372 emissions. The largest five Hg emission provinces were Hebei, Shandong, Henan, Jiangsu,
373 and Shanxi provinces. Emissions from these provinces reached 21.5 t, accounting for 68% of
374 national emissions.

375 With better understanding of Hg flow in ISP, the uncertainty of atmospheric Hg
376 emissions from ISP estimated by using technology-based emission factor model has largely
377 reduced. However, with the continuously change of APCD combinations, extensive and
378 dedicated field experiments are still required to generate suitable database of Hg removal
379 efficiencies for the improved APCDs in the future.

380 *Acknowledgment.* This study was supported by the Major State Basic Research Development
381 Program of China (973 Program) (2013CB430001), Natural Science Foundation of China
382 (21607090), and China Postdoctoral Science Foundation (2016T90103, 2016M601053)

383



384 **References**

- 385 Arctic Monitoring and Assessment Programme and United Nations Environment Programme
386 (AMAP/UNEP): Technical background report to the global atmospheric mercury
387 assessment, AMAP/UNEP, Geneva, Switzerland, 2008.
- 388 Arctic Monitoring and Assessment Programme and United Nations Environment Programme
389 (AMAP/UNEP): Technical background report for the global mercury assessment,
390 AMAP/UNEP, Geneva, Switzerland, 2013.
- 391 China Iron and Steel Industry Association (CISIA): China Steel yearbook, CISIA, Beijing,
392 China, 2001-2016.
- 393 China Iron and Steel Industry Association (CISIA): China Steel yearbook, CISIA, Beijing,
394 China, 2016.
- 395 European Monitoring and Evaluation Programme/Core Inventory of Air Emissions Project
396 (EMEP/CORINAIR): Emission inventory guidebook, EMEP/CORINAIR, Copenhagen,
397 Denmark, 2001.
- 398 European Monitoring and Evaluation Programme/European Economic Area (EMEP/EEA):
399 Air pollutant emission inventory guidebook 2013, EMEP/EEA, Copenhagen, Denmark,
400 2013.
- 401 Gao, W.: Study on Atmospheric Mercury Emission Characteristics for Iron and Steel
402 Producing Process in China, Tsinghua University, School of Environment, Beijing, China,
403 2016.
- 404 Guo, T., and Wei, L.: Development direction of the recycling industry of secondary zinc
405 resources, China Nonferrous Metall., 4, 2010.
- 406 Hui, M. L., Wu, Q. R., Wang, S. X., Liang, S., Zhang, L., Wang, F. Y., Lenzen, M., Wang, Y.
407 F., Xu, L. X., Lin, Z. T., Yang, H., Lin, Y., Larssen, T., Xu, M., and Hao, J. M.: Mercury
408 Flows in China and Global Drivers, Environ. Sci. Technol., 51, 222-231, 2016.
- 409 Li, X. C., Gao, X., and Jiang, X. D.: Analysis on potential of energy conservation of Chinese
410 steel industry in the 13th five-year period, The tenth annual conference of China steel
411 and the sixth annual academic conference of Baogang, Shanghai, Beijing, 2015-10-21,
412 2015.



- 413 Ma, H. L.: China steel statistics, Development and Planning Division of Ministry of
414 Metallurgical, Beijing, China, 1995.
- 415 Ma, J.: Review and projection of technology development of lime used in China's steel
416 industry, China steel, 6, 17-20, 2011.
- 417 Ministry of Environmental Protection (MEP): "Twelfth Five-year" plan for the comprehensive
418 prevention and control of heavy metal pollution, MEP, Beijing, China, 2011.
- 419 Ministry of industry and information Technology (MIIT): Adjustment and upgrading plan of
420 iron and steel industry (2016-2020), MIIT, Beijing, China, 2016.
- 421 National Statistical Bureau of China (NBS): China Environmental Statistics Yearbook, NBS,
422 Beijing, China, 2001-2016.
- 423 National Energy Administration (NEA): Action plan of coal clean utilization, NEA, Beijing,
424 China, 2014.
- 425 National energy statistical agency of China (NESA): China Energy Statistical Yearbook,
426 NESA, Beijing, China, 2001-2016.
- 427 State Council of the People's Republic of China (SC): Action plan of national air pollution
428 prevention and control, SC, Beijing, China, 2013.
- 429 Streets, D. G., Hao, J. M., Wu, Y., Jiang, J. K., Chan, M., Tian, H. Z., and Feng, X. B.:
430 Anthropogenic mercury emissions in China, Atmos. Environ., 39, 7789-7806, 2005.
- 431 Swaine, D. J.: Environmental Aspects of Trace-Elements in Coal, Environ. Geochem. Health,
432 14, 2-2, 1992.
- 433 Tao, S. R., and Wang, Y. J.: Impact on the economic benefits of metallurgy industry from
434 coke coal quality, Coal Proce. Compre. Utiliz., 4, 1994.
- 435 Tian, H. Z., Wang, Y., Xue, Z. G., Cheng, K., Qu, Y. P., Chai, F. H., and Hao, J. M.: Trend and
436 characteristics of atmospheric emissions of Hg, As, and Se from coal combustion in
437 China, 1980-2007, Atmos. Chem. Phys., 10, 11905-11919, 2010.
- 438 Tian, H. Z., Zhu, C. Y., Gao, J. J., Cheng, K., Hao, J. M., Wang, K., Hua, S. B., Wang, Y., and
439 Zhou, J. R.: Quantitative assessment of atmospheric emissions of toxic heavy metals
440 from anthropogenic sources in China: historical trend, spatial distribution, uncertainties,
441 and control policies, Atmos. Chem. Phys., 15, 10127-10147, 2015.



- 442 United Nations Environment Programme (UNEP): Toolkit for identification and
443 quantification of mercury releases. Guideline for Inventory Level 2, Version 1.3. , 2013.
- 444 United States Environmental Protection Agency (US EPA): Method 7473: Hg in solids and
445 solutions by thermal decomposition amalgamation and atomic absorption
446 spectrophotometry, US EPA, Washington D. C., United States, 1998.
- 447 United States Geological Survey (USGS): Mercury content in coal mines in China, Reston,
448 Virginia, United States, 2004.
- 449 Wang, F. Y., Wang, S. X., Zhang, L., Yang, H., Gao, W., Wu, Q. R., and Hao, J. M.: Mercury
450 mass flow in iron and steel production process and its implications for mercury emission
451 control, *J. Environ. Sci.*, 43, 293-301, 2016.
- 452 Wang, K., Tian, H. Z., Hua, S. B., Zhu, C. Y., Gao, J. J., Xue, Y. F., Hao, J. M., Wang, Y., and
453 Zhou, J. R.: A comprehensive emission inventory of multiple air pollutants from iron and
454 steel industry in China: Temporal trends and spatial variation characteristics, *Sci. Total
455 Environ.*, 559, 7-14, 2016.
- 456 Wang, S. X., Zhang, L., Li, G. H., Wu, Y., Hao, J. M., Pirrone, N., Sprovieri, F., and Ancora,
457 M. P.: Mercury emission and speciation of coal-fired power plants in China, *Atmos.
458 Chem. Phys.*, 10, 1183-1192, 2010.
- 459 Wang, S. X., Zhao, B., Cai, S. Y., Klimont, Z., Nielsen, C. P., Morikawa, T., Woo, J. H., Kim,
460 Y., Fu, X., Xu, J. Y., Hao, J. M., and He, K. B.: Emission trends and mitigation options
461 for air pollutants in East Asia, *Atmos. Chem. Phys.*, 14, 6571-6603, 2014.
- 462 Wang, Y. F.: Analysis on the harm of indigenous coking, *Coal Eco. Res.*, 1, 1991.
- 463 Wu, Q., Wang, S., Li, G., Liang, S., Lin, C.-J., Wang, Y., Cai, S., Liu, K., and Hao, J.:
464 Temporal Trend and Spatial Distribution of Speciated Atmospheric Mercury Emissions
465 in China During 1978–2014, *Environ. Sci. Technol.*, 50, 13428-13435, 2016.
- 466 Wu, Q. R., Wang, S. X., Zhang, L., Song, J. X., Yang, H., and Meng, Y.: Update of mercury
467 emissions from China's primary zinc, lead and copper smelters, 2000-2010, *Atmos.
468 Chem. Phys.*, 12, 11153-11163, 2012.
- 469 Wu, S. H.: Interpretation about “Emission Standards of Iron and Steel Industrial Pollutants”,
470 *Indus. Safety Environ. Pro.*, 29, 2, 2013.



- 471 Wu, Y., Wang, S. X., Streets, D. G., Hao, J. M., Chan, M., and Jiang, J. K.: Trends in
472 anthropogenic mercury emissions in China from 1995 to 2003, *Environ. Sci. Technol.*, 40,
473 5312-5318, 2006.
- 474 Zhang, L.: Emission characteristics and synergistic control strategies of atmospheric mercury
475 from coal combustion in China, Ph.D. Dissertation, Tsinghua University, School of
476 Environment, Beijing, China, 2012.
- 477 Zhang, L., Wang, S. X., Meng, Y., and Hao, J. M.: Influence of mercury and chlorine content
478 of coal on mercury emissions from coal-fired power plants in China, *Environ. Sci.*
479 *Technol.*, 46, 6385-6392, 2012.
- 480 Zhang, L., Wang, S. X., Wang, L., Wu, Y., Duan, L., Wu, Q. R., Wang, F. Y., Yang, M., Yang,
481 H., Hao, J. M., and Liu, X.: Updated emission inventories for speciated atmospheric
482 mercury from anthropogenic sources in China, *Environ. Sci. Technol.*, 49, 3185-3194,
483 2015.
- 484 Zhang, Y. H., Zhang, C., Wang, D. Y., Luo, C., Yang, X., and Xu, F.: Characteristic of
485 mercury emissions and mass balance of the typical iron and steel industry, *Environ. Sci.*,
486 36, 8, 2015.
- 487 Zhao, B., Wang, S. X., Liu, H., Xu, J. Y., Fu, K., Klimont, Z., Hao, J. M., He, K. B., Cofala, J.,
488 and Amann, M.: NO_x emissions in China: historical trends and future perspectives,
489 *Atmos. Chem. Phys.*, 13, 9869-9897, 2013.
- 490



491 **Tables**

492 Table 1. Hg concentration in the raw materials

Province ¹	Iron ore			Limestone			Dolomite			Coking coal			PCI coal				
	AM ² ng/g	MV ² ng/g	SV ² ng/g	NS ²	AM ng/g	MV ng/g	SV ng/g	NS	AM ng/g	MV ng/g	SV ng/g	NS	AM ng/g	MV ng/g	SV ng/g	NS	
Tianjin	41	44	8	3	9	9	3	1	5	5	2	4	75	66	31	5	
Hebei	37	24	40	79	374	117	631	27	7	8	5	5	78	66	39	71	85
Shanxi	30	24	28	25	9	7	8	6					77	71	27	22	114
Shanghai	44	44	50	4	20	20	5	1	39	39	2	2	125	152	71	5	12
Jiangsu					103	68	113	18									
Zhejiang					52	37	35	22									
Anhui	21	20	12	14	11	11	4	12	32	32	2	3	88	58	53	8	98
Fujian	19	14	11	15	11	11	5	4	9	8	5	4	105	100	51	13	255
Jiangxi	57	46	88	18					10	9	4	3	120	93	59	4	185
Shandong	125	128	73	20					24	24	1	2	72	69	21	12	
Henan	32	24	29	18	692	759	629	13									
Hubei					16	14	8	6					92	83	54	39	131
Human	33	19	34	77	102	87	62	4	3	3	1	2					
Guangdong					48	44	26	15									
Guangxi					8	8	2	4					210	188	112	27	96
Chongqing													85	79	48	20	65
Sichuan	37	2	44	7	10	9	4	12									
Guizhou					11	10	11	42									
Yunnan	10	10	7	6	17	20	7	6					51	52	7	8	58



Gansu	107	107	3	3	3	3	1	1	1	166	174	21	5	60	60	5	2
Xinjiang	6	5	4	17						82	82	46	22	31	24	19	15
National	38	20	48	306	153	18	402	204	14	9	12	25	256	99	73	83	120

493 Note: 1. Provinces without data were not listed in this table;

494 2. AM: Average mean; MV: Median value; SV: Standard value; NM: Number of samples.



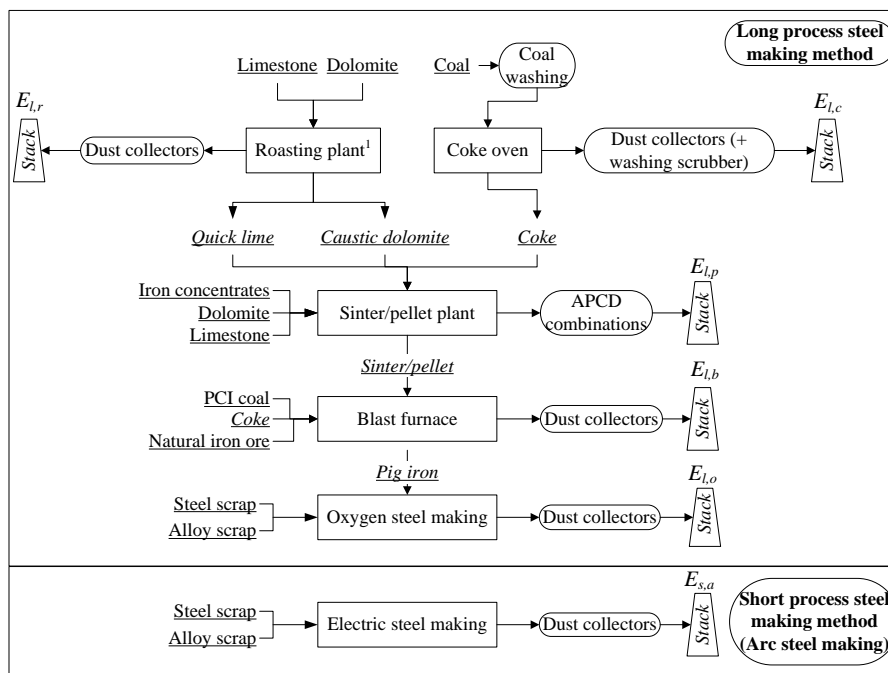
495 Table 2. Provincial Hg emissions during 2000-2015

Province	Atmospheric Hg emissions (t)				
	2000	2005	2010	2015	AAGR
Beijing	0.4	0.3	0.1	0.0	-40%
Tianjin	0.3	0.5	0.9	0.7	7%
Hebei	1.2	4.0	6.7	7.1	13%
Shanxi	1.6	2.2	2.1	1.8	1%
Inner Mongolia	0.3	0.5	0.7	0.8	7%
Liaoning	0.8	1.2	1.7	1.6	4%
Jilin	0.1	0.2	0.3	0.3	6%
Heilongjiang	0.1	0.2	0.3	0.2	6%
Shanghai	1.5	1.2	1.0	0.7	-5%
Jiangsu	0.3	1.1	1.9	2.5	15%
Zhejiang	0.1	0.1	0.4	0.4	11%
Anhui	0.3	0.4	0.6	0.6	6%
Fujian	0.1	0.2	0.2	0.3	11%
Jiangxi	0.3	0.7	1.1	1.0	8%
Shandong	1.1	4.0	6.0	6.1	12%
Henan	1.3	2.2	3.5	4.0	8%
Hubei	0.3	0.4	0.5	0.4	2%
Hunan	0.2	0.5	0.7	0.6	7%
Guangdong	0.1	0.3	0.3	0.4	8%
Guangxi	0.1	0.2	0.4	0.5	13%
Hainan	0.0	0.0	0.0	0.0	26%
Chongqing	0.1	0.1	0.2	0.1	2%
Sichuan	0.2	0.4	0.4	0.4	4%
Guizhou	0.1	0.2	0.2	0.2	4%
Yunnan	0.1	0.3	0.4	0.3	7%
Tibet	0.0	0.0	0.0	0.0	/
Shaanxi	0.1	0.2	0.4	0.7	16%
Gansu	0.4	0.5	0.6	0.7	4%
Qinghai	0.0	0.0	0.1	0.0	5%
Ningxia	0.0	0.0	0.1	0.1	19%
Xinjiang	0.1	0.1	0.3	0.3	13%
Total	11.5	22.2	31.9	32.7	7%

496

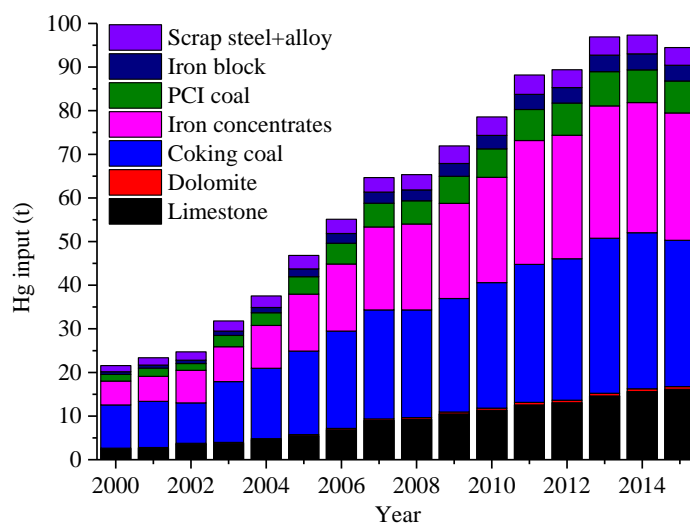


497 **Figures**



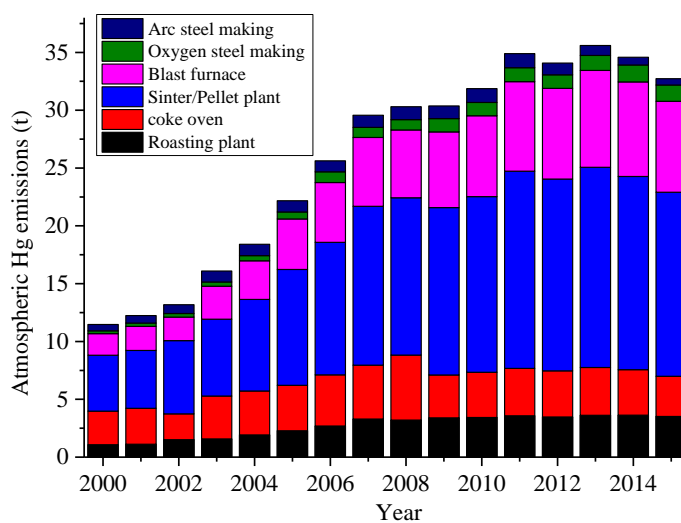
498

499 **Fig. 1.** Flow chart of ISP processes (1. Some plants roasted limestone and dolomite separately.)



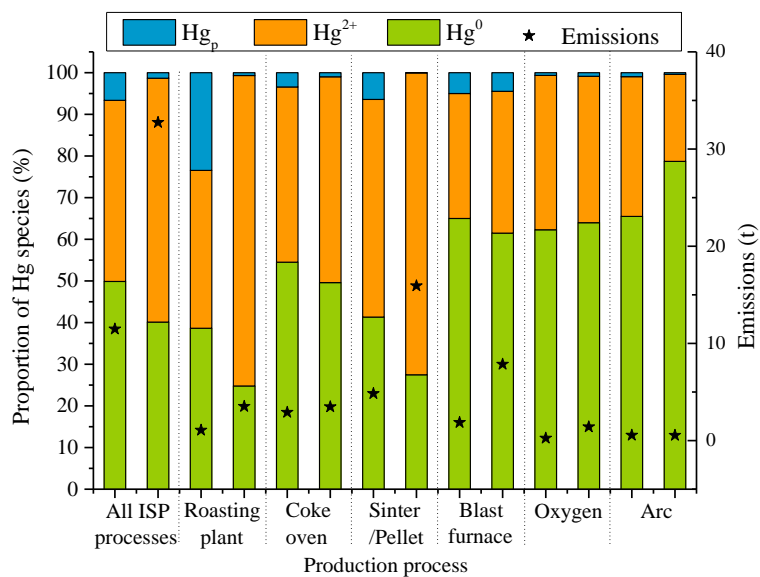
500

501 **Fig. 2.** Hg input trends by material



502

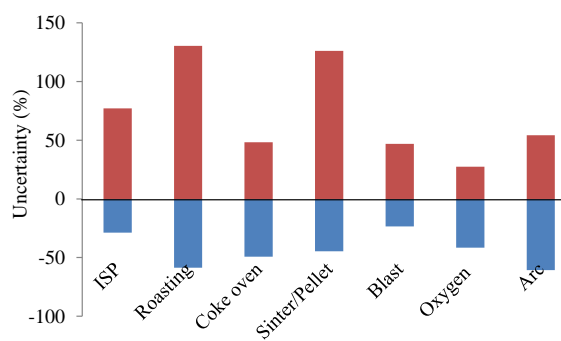
503 **Fig. 3.** Hg emission trends by process



504

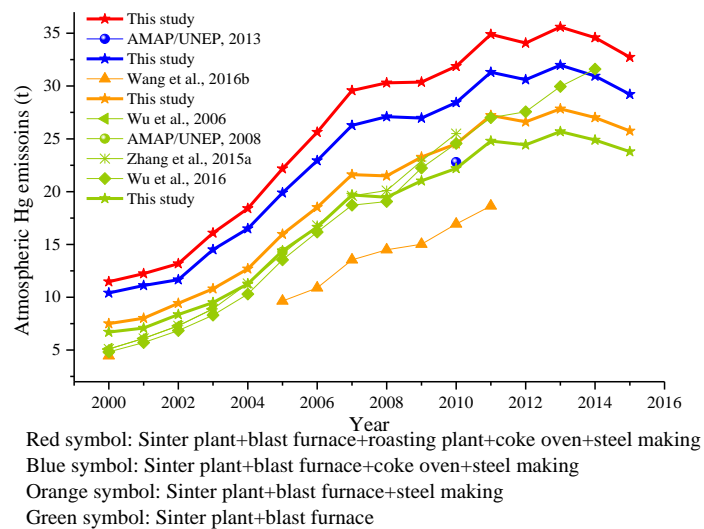
505 **Fig. 4.** Proportion of different Hg species (For each process, the left and right column

506 represents the data in 2000 and 2015, respectively)



507

508 **Fig. 5.** Unertainty analysis



509

510 **Fig. 6.** Atmospheric Hg emissions of ISP in different studies

511